The Effect of Pre-Impact Topography on Ray Production for Lunar Copernican Craters

K. S. Martin-Wells[1] and J. Partee[1], [1]Ursinus College (Pfahler Hall, 601 E. Main Street, Collegeville, PA 19426. kmartinwells@ursinus.edu)

Introduction: Investigations of lunar crater rays have revealed key insights not only into the formation and preservation of rays themselves, but also the role that rays play in distributing and mixing primary ejecta with local material [e.g., 1-6]. As such, an understanding of lunar rays is essential to understanding the evolution of the surface not only of the Moon, but other airless bodies. Sabuwala et al. [2018] determined a relationship between the topography of pre-impact surfaces in granular cratering experiments and the number of rays of the resulting craters [7]. In this work, we investigate the extent to which this trend is measurable in actual lunar impact craters.

	Crater Diameter (km)	Predicted Impactor Diameter (km)
Tharp	13.5	1.0
Mandel'shtam F	15.4	1.1
Ventris M	17.5	1.3
Byrgius A	18.5	1.4
Giordano Bruno	22.1	1.7
Larmor Q	23.0	1.7
Proclus	26.9	2.1
Kepler	29.5	2.3
Aristarchus	40.0	3.2
Glushko	40.1	3.2
Wiener F	44.9	3.6
Ohm	61.8	5.1
Jackson	71.4	6.0
Tycho	85.3	7.3
Copernicus	96.1	8.3

Table 1. Copernican-aged craters selected for investigation. Impactor diameters calculated using Equation (1).

Background: Combining low-velocity granular cratering experiments and simulations of hyper-velocity impacts into granular targets, Sabuwala et al. [2018] addressed a long-standing puzzle in granular cratering experiments—what could account for the lack of prominent rays produced, and what could their absence tell us about the origin of rays in the impact cratering process? They observed a linear relationship between the wavelength of undulation of the pre-impact surface, λ, the size of the impactor, D, and the number of prominent rays observed, N [7]. By observing impacts into pre-impact surfaces with regular, hexagonal depressions of wavelength, λ, their experiments produced N prominent rays [7]. Sabuwala et al. [2018] proposed a simple geometric model to explain the dependence of N on the dimensionless ratio, D/ λ. By tracing the paths of granules in their hyper-velocity simulations, Sabuwala et al. [2018] found that the particles which formed prominent rays originated from a narrow annulus straddling the edge of the impacting ball during the early-time interaction of the impactor with the target. They found that the number of low-points ("prominent valleys"), N_v, where this pre-impact target topography intersected with the edge of the impacting ball explained the number of resulting prominent rays, with $N = N_v$.

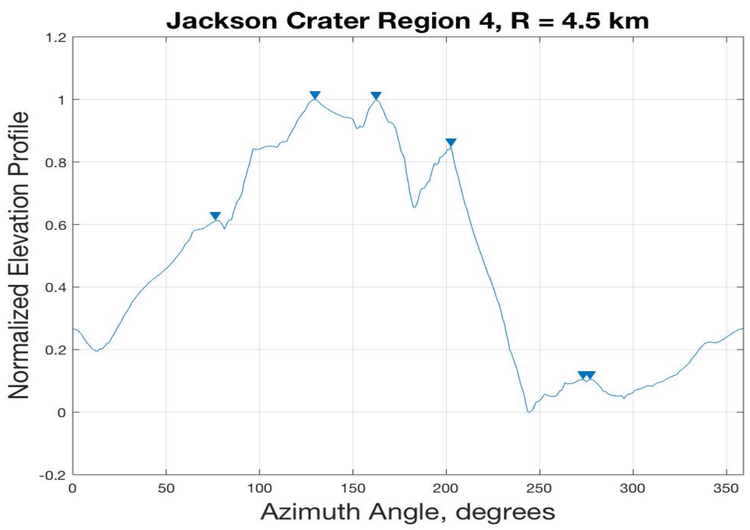

Figure 1. Normalized elevation profile from a 10 x 10 km^2 patch ("Region 4") of topography extracted in the annulus surrounding Jackson crater. This profile was taken along a circular profile with a radius, R = 4.5 km, from the center of the patch. This would correspond with a hypothetical impactor diameter of D = 9 km for Jackson. The MATLAB function *findpeaks()* was used to identify the six prominent valleys (shown here as peaks in the inverted data). The *MinPeakProminence* parameter was set to 0.02 for the data shown.

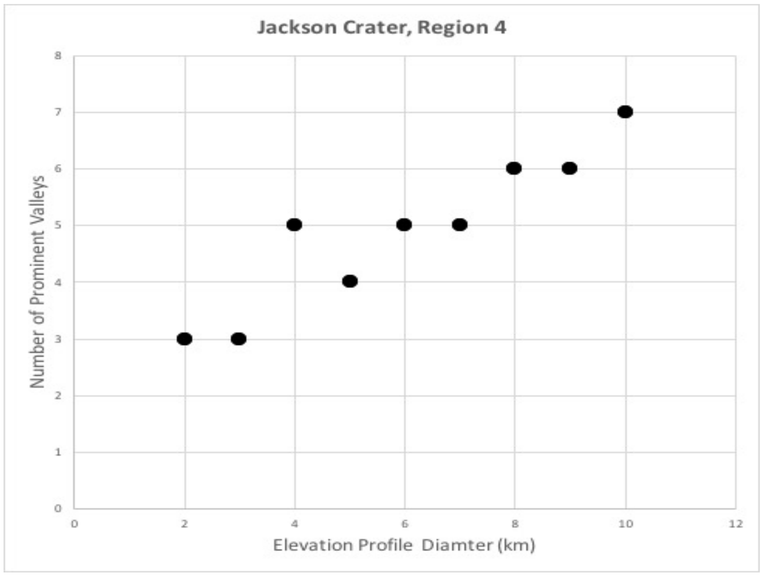

Figure 2. Elevation profile diameter vs. number of prominent valleys measured for Jackson crater, Region 4. After averaging 75 of these profile diameter vs. N_v measurements for each crater, the diameter of the impactor is inferred to be the diameter of the elevation profile with a corresponding number of prominent valleys equal to the number of prominent rays of the crater ($N_v = N$). The *MinPeakProminence* parameter was set to 0.02 for the data shown.

Data Collection: We have identified sixteen lunar craters of Copernican age with diameters ranging from 10 – 100 km. The expected impactor diameter for each crater was calculated using Cintala and Grieve [1998]'s gravity regime scaling law [8]:

$$D_r = 0.828\, D_{sc}^{\ 0.20} \left(\frac{\rho_p}{\rho_t}\right)^{0.39} d_p^{\ 0.92}\, v_i^{\ 0.52}\, g^{-0.26} \quad \textbf{(1)}$$

Where D_r is the impactor diameter, D_{sc} is the simple-to-complex crater transition diameter; ρ_p and ρ_t are the projectile and target densities, respectively; d_p is the final crater diameter, v_i is the impactor velocity, and g = 1.6 m/s^2 for the moon [8]. Here we have assumed that D_{sc} = 18 km, $\rho_p = \rho_t$, and v_i = 15 km/s. The impactor diameters predicted by this scaling law are presented in Table 1. According to Sabuwala et al. [2018]'s model, the number of rays of the resulting crater is controlled by the number of prominent valleys touching the diameter of the projectile at impact. Thus, by measuring the number of prominent rays of each of these craters, we are inferring the number of prominent valleys located along a circle of radius equal to one projectile radius from the point of impact. We imagine that the contact between the topography and various-sized projectiles is represented by the circular topographic profiles. Whichever profile best fits the observed number of rays, then, is the inferred projectile diameter. Sabuwala et al. [2018] used this method to infer d = 3.4 km for Kepler and d = 11 km for Tycho crater, using a MATLAB *MinPeakProminence* value set to 0.05.

Following the procedure of Sabuwala et al. [2018], regions for extracting elevation profiles were selected in annuli between 1.5 and 2 crater diameters from the center of the crater. Regions closer to the crater were not used in order to avoid the continuous ejecta blanket. From within this annulus, 10 x 10 km^2 regions were selected out of which to extract the elevation profiles. Each 10 x 10 km^2 patch, ideally, would be representative of the pre-impact target surface. However, to account for local variation in topography, data from 75 patches with in the annulus are averaged for each crater. Following the method of Sabuwala et al. [2018], elevation profiles were taken along circular paths, each concentric to the patch center. These paths have radii ranging from R = 1 to 5 km, at 0.5 km increments. The elevation profiles in this work were derived from LOLA 1024ppd numeric elevation data using the JMars software [9]. Elevation was extracted every 75 m along each circular path to construct the topographic profiles. To determine the number of prominent valleys along each circular elevation profile, we followed the method outlined in Sabuwala et al. [2018], using the MATLAB function, *findpeaks()*. First, the data were inverted so that the valleys were represented as peaks. Profiles were also normalized to a maximum elevation value of 1 and a minimum of 0 before the *findpeaks()* function was applied (Figure 1). Data-taking for our 16 Copernican craters is ongoing (Figure 2).

References: [1] Shoemaker E. M. (1966) Preliminary analysis of the fine structure of the lunar surface in Mare Cognitum. In: Hess, W.N., Menzel, D.H., O'Keefe, J.A. (Eds.), The Nature of the Lunar Surface. Johns Hopkins Press, Baltimore, pp. 23-77. [2] Oberbeck V. R. (1971) *Moon* 2, 263-278. [3] Oberbeck V. R. (1975) *Rev. Geophys. Space Phys*., 13,337-362. [4] Morrison R.H. and Oberbeck V. R. (1975). Geomorphology of crater and basin deposits: emplacement of the Fra Mauro formation. In: *Proc. Lunar Planet. Sci. Conf.* 6th, pp. 2503-2530. [5] Pieters C. M. et al. (1985) *JGR*, *90*,12393-12413. [6] Hawke B. R. et al. (2004) *Icarus*, 170, 1-16. [7] Sabuwala et al. (2018) *PRL*, 120, 264501. [8] Cintala M. J. and R. A. F. Grieve (1998) *Meteoritics & Planet. Sci.,* 33, 889-912. [9] Christensen et al. (2009) *AGU Fall Meeting Abstracts*, IN22A-06.